

# Parkinsonian Tremor as Unstable Feedback in a Physiologically Consistent Control Framework

Christopher R. Kelley and Jeffrey L. Kauffman

Abstract—Parkinson's disease (PD) is characterized by decreased dopamine in the basal ganglia that causes excessive tonic inhibition of the thalamus. This excessive inhibition seems to explain inhibitory motor symptoms in PD, but the source of tremor remains unclear. This paper investigates how neural inhibition may change the closed-loop characteristics of the human motor control system to determine how this established pathophysiology could produce tremor. The rate-coding model of neural signals suggests increased inhibition decreases signal amplitude, which could create a mismatch between the closed-loop dynamics and the internal models that overcome proprioceptive feedback delays. This paper aims to identify a candidate model structure with decreasedamplitude-induced tremor in PD that also agrees with previously recorded movements of healthy and cerebellar patients. The optimal feedback control theory of human motor control forms the basis of the model. Key additional elements include gating of undesired movements via the basal ganglia-thalamus-motor cortex circuit and the treatment of the efferent copy of the control input as a measurement in the state estimator. Simulations confirm the model's ability to capture tremor in PD and also demonstrate how disease progression could affect tremor and other motor symptoms, providing insight into the existence of tremor and non-tremor phenotypes. Altogether, the physiological underpinnings of the model structure and the agreement of model predictions with clinical observations provides support for the hypothesis that unstable feedback produces parkinsonian tremor. Consequently, these results also support the associated framework for the neuroanatomy of human motor control.

*Index Terms*—Tremor, Parkinson's disease, control, feedback.

## I. INTRODUCTION

THE human motor system produces voluntary movements through some combination of feedback and model-based control [1], [2], [3]. Sensory feedback takes time to travel from sensory receptors to the central nervous system (CNS) and back to muscles: typical closed-loop feedback delays are

Manuscript received 5 February 2024; revised 26 June 2024; accepted 15 July 2024. Date of publication 17 July 2024; date of current version 26 July 2024. This work was supported in part by the National Science Foundation under Grant 2346917. (Corresponding author: Christopher R. Kelley.)

Christopher R. Kelley is with the Mechanical Engineering Department, Florida Polytechnic University, Lakeland, FL 33805 USA (e-mail: ckelley@floridapoly.edu).

Jeffrey L. Kauffman is with the Mechanical and Aerospace Engineering Department, University of Central Florida, Orlando, FL 32816 USA (e-mail: JLKauffman@ucf.edu).

Digital Object Identifier 10.1109/TNSRE.2024.3430116

on the order of 50-100 ms [4]. This delay is too high to execute stable feedback control directly from measurements; however, the CNS uses internal models to predict future states and enable feedback with effectively zero delay [5]. Significantly, the accuracy of these internal models affects controller stability [6]. Pathological tremor is the undesired, approximately rhythmic movement of body parts—this oscillatory movement resembles unstable feedback with control input saturation [7], [8]. However, most research towards understanding pathological tremor investigates physiological aspects of tremor generation like neural activity rather than aiming to understand the system-level dysfunction. This paper explores a contrasting fundamental question: can control-system roles of brain regions and the control-system dysfunction of movement disorder pathophysiology mutually inform each other to improve our understanding of both?

The key movement disorder feature addressed in this work is tremor in Parkinson's disease (PD). Dopamine depletion in the basal ganglia is a defining characteristic of PD [9]. This decreased dopamine shifts the balance of basal ganglia output to the thalamus towards inhibition: the internal portion of the globus pallidus (GPi) projects excessive tonic inhibition to the anterior portion of the ventral lateral thalamus (VLa). Naturally, excessive inhibition of the motor thalamus is thought to play a critical role in the increased reaction times and slowness of movement that are characteristic motor symptoms in PD [10]. Recent research demonstrates reduced motor vigor in PD, while motor vigor models provide insight into how reduced dopamine may affect system-level parameters [11], [12]. However, the pathophysiology of parkinsonian tremor is less clear: how does excessive inhibition translate to undesired motion? The overarching hypothesis of this work is that excessive tonic inhibition from GPi to VLa produces unstable feedback in PD. Significantly, this theory implies a single physiological mechanism (excessive inhibition of VLa) can produce both tremor and movement inhibition in PD.

In contrast to this approach, existing theories for parkinsonian tremor pathophysiology do not link tremor to inhibitory movement symptoms; current leading theories include pacemaker and dimmer-switch hypotheses [13]. Pacemaker hypotheses suggest tremor originates from oscillatory cells in the basal ganglia or thalamus, but they fail to address how deep brain stimulation (DBS) targeting either region reduces tremor [13]. The dimmer-switch hypothesis identifies roles for both regions, suggesting the basal ganglia triggers tremor while the cerebello-thalamo-cortical (CTC) circuit drives tremor [9]. Overall, these theories use neural activity observed in clinical studies to identify possible drivers of tremor, but do not address the cause of dysfunction explicitly.

The neuroanatomy of motor control provides insight into how PD pathophysiology may affect the control system. Key general regions for motor control are the motor cortex, parietal cortex, cerebellum, and basal ganglia. Shadmehr and Krakauer [14] applied evidence from movement studies to develop a prospective framework for motor control that leverages the optimal feedback control theory of human movement introduced by Todorov and Jordan [15]. In their framework, the basal ganglia determines the cost and reward structure of the task, the motor cortex implements feedback control given a state estimate, and the parietal cortex produces the state estimate given sensory measurements along with forward predictions from the cerebellum. This general framework remains the leading high-level system model for motor control, with recent work extending the model to include additional behavior [8], [16], [17], [18].

The standard computational neuroanatomy framework cannot capture the excessive inhibition of the thalamus from the basal ganglia in PD. Indeed, these types of studies often overlook the role of the thalamus, but it is a critical piece of PD pathophysiology. The thalamus relays signals among the basal ganglia, cerebellum, and cortex, possibly integrating signals or performing other computations along the way [19]. Thus, excessive inhibition of the thalamus likely affects activity of the cortex and cerebellum. The "gating" model captures one potential mechanism of basal ganglia control of thalamus activity: GPi suppresses VLa activity to prevent undesired movements and allows desired movements through disinhibition [19], [20]. Many studies indicate the basal ganglia is involved in motor response inhibition and selecting among competing motor programs [21]. Integrating the gating model into the computational neuroanatomy framework could identify how excessive inhibition produces tremor in PD. However, the vast interconnectivity among brain regions makes including this component nontrivial.

Recently, the authors and other researchers modeled uncompensated delays as a mechanism of unstable feedback stemming from excessive inhibition [7], [8], [22], [23]. While simulations and model structure generally agree with clinical observations, it is unclear how excessive inhibition could produce a signal delay. This paper presents another possible mechanism for unstable feedback: mismatch between internal models and actual dynamics due to decreased signal levels. Tonic inhibition decreasing signal levels has a much more straightforward physiological underpinning: lower firing rates represent lower signals for rate-coded information [24], [25], [26]. This signal distortion can cause unstable feedback when forward predictions become out-of-phase with the actual state dynamics. Overall, the need for model-based delay compensation is a key component for the potential to produce unstable feedback. However, the dysfunction does not have to be a change in the delay value, but any change that causes a mismatch between the internal model and actual dynamics. While [14] acknowledges the existence of a sensory delay, the implemented model does not address delay compensation. This factor is a key element included in this work.

Similar to delay-induced tremor, the tremor theory in this work (and likely any theory based on unstable feedback)

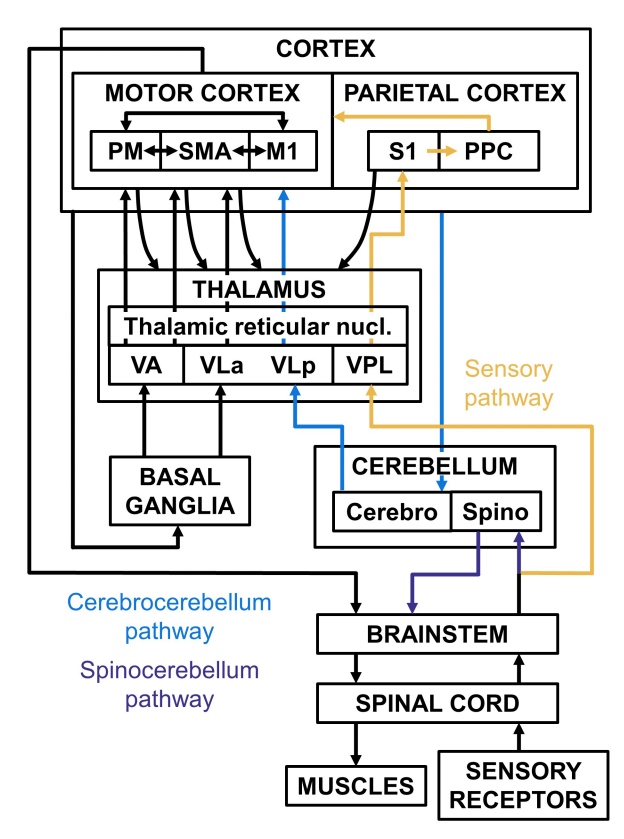


Fig. 1. Sensory feedback may take many pathways through the CNS.

meshes well with the observations that motivate the dimmerswitch hypothesis [8]. Considering the anatomical connections among brain regions and their prospective control-system roles facilitates the development of a new candidate motor control model that includes the key elements for parkinsonian tremor. Altogether, this paper centers about two primary contributions. First, this study identifies potential control-system dysfunction mechanisms in PD to develop a new control-system framework of human motor control. Key additions to the standard computational neuroanatomy framework include the basal ganglia gating model and the inclusion of the efferent copy of the control input as a measurement in the state estimation process. Second, the evaluation of model predictions provides insight into the characteristics of PD and computational support for the candidate model.

#### II. TONIC INHIBITION AND UNSTABLE FEEDBACK

The first step in modeling the hypothesis that excessive GPi inhibition of VLa causes unstable feedback in PD is identifying *where* the pathological behavior affects the control system. Figure 1 illustrates some of the key pathways involved in human motor control to provide insight into this question. Note that the motor cortex regions include the primary motor cortex (M1), supplementary motor area (SMA), and premotor cortex (PM) while key parietal cortex regions include the primary somatosensory area (S1) and the posterior parietal cortex (PPC). In addition to VLa, the key thalamus regions include the ventral anterior nucleus (VA), the posterior portion of the ventral lateral nucleus (VLp), the ventral posterolateral nucleus (VPL), and the thalamic reticular nucleus (TRN).

CNS processing of proprioceptive feedback takes two pathways: one through the spinocerebellum and another beginning

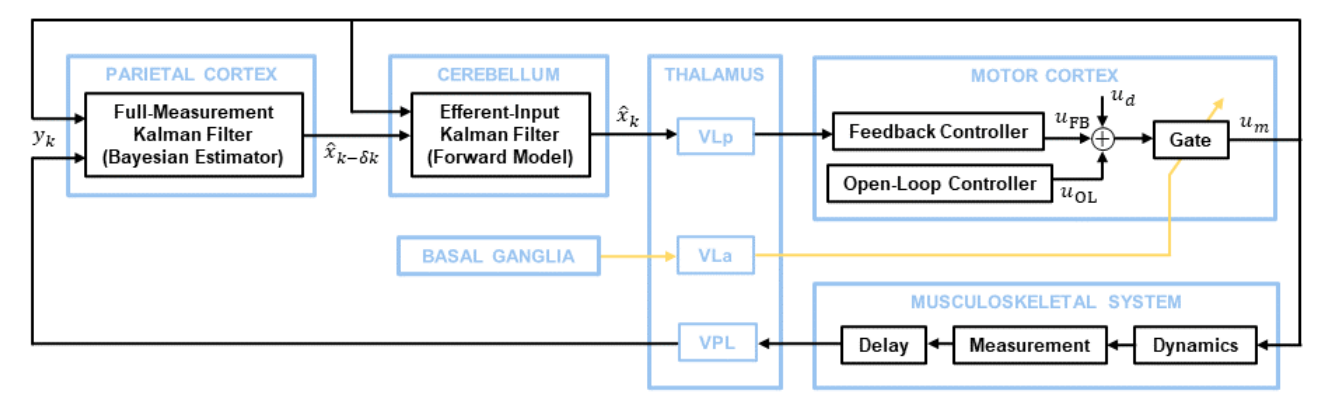


Fig. 2. Block diagram of the candidate human motor control model with tremor in PD generated by a decreased gate value.

at VPL and continuing to S1 [27]. The spinocerebellum pathway sends signals directly to the brainstem, enabling input to effectors. From S1, the feedback signal may take a number of pathways before producing effector inputs at the motor cortex: through the PPC, the cerebrocerebellum pathway, the thalamus, or directly to the motor cortex. The interconnectivity of these regions makes it difficult to identify complete pathways: virtually all cortex regions are connected, thalamocortical radiations and the TRN enable connections across the thalamus and cortex, and the cerebellum receives input from multiple cortical areas [27]. Excessive inhibition of VLa may affect these pathways by

- 1) Changing VLa excitation of the motor cortex.
- Spreading inhibition to VLp via the TRN, thereby changing VLp excitation of the motor cortex.
- Spreading inhibition to VPL via the TRN, thereby changing VPL excitation of S1.

The variety of hypothesized roles of brain regions further obscures the potential locations of PD pathology in control-system models. A key factor to produce unstable feedback is the use of forward models for fast feedback control that overcomes sensory delays. However, studies link forward models to the cerebellum, parietal cortex, and primary motor cortex, obscuring where PD pathology may exist relative to forward models [5], [14], [28]. The three excessive inhibition theories described above applied to the model of Shadmehr and Krakauer [14] would change the signal near the feedback controller, after the forward model, and before the forward model, respectively.

Given potential locations, the next step is identifying *how* the pathological behavior affects the control system. Recall, the key pathology is excessive tonic inhibition of VLa. This tonic inhibition affects ambient GABA concentration that ultimately increases membrane conductance, thereby decreasing the membrane time constant [29]. For a typical integrate-and-fire neuron system, decreasing the membrane time constant decreases the firing rate [30]. For rate-coded signals, lower firing rates are equivalent to decreased signal amplitudes [24]. This fact points towards the effect of excessive tonic inhibition on VLa being a decrease in a signal amplitude somewhere in the control system. Further specification of the location and role of excessive inhibition of VLa is not easily defined from existing CNS knowledge and is the key task addressed in the following section.

#### III. CANDIDATE MODEL

The goal of the following candidate model is to capture both healthy and pathological movement characteristics while retaining consistency with human neuroanatomy. Figure 2 illustrates the block diagram for the model including control-system components and associated physiological structures. The model is mostly inspired by the neuroanatomy framework of Shadmehr and Krakauer [14], but slightly increases the resolution of system roles to capture all of the targeted behavior. The parietal cortex and cerebellum implement Kalman filters that produce an estimate of the current state given delayed measurements and efferent copies of the control input. The motor cortex implements feedback control using this state estimate, but also includes an open-loop component to enable fast responses to known dynamics without waiting for delayed measurements. The complete feedback pathway could be a combination of the sensory and cerebrocerebellum pathways in Fig. 1. The PPC sends processed sensory information to the cerebellum for forward predictions. The cerebellum sends the forward predictions to the cortex for feedback control that enables an adaptive response to disturbances and unknown dynamics.

Two key components enable modeling of tremor in PD. First, the model includes a "gate" based on the basal ganglia gating model. Tasks are gated by basal ganglia input: in the healthy state, the gate is either open or closed, facilitating and blocking desired and undesired movements, respectively. In PD, the gate "opens" only partially, decreasing the signal. Second, the Kalman filters treat the descending control input as a state measurement. The model assumes the "known" control input in the filter equations is known because the cerebellum and parietal cortex know the feedback gains, not because it is supplied by the efferent copy of the motor cortex output. The efferent copy of the motor cortex output enables rapid compensation for control input disturbances. This structure allows the healthy control system to overcome variations in control input without waiting for delayed measurements. However, it also produces a mismatch between internal model and actual parameters in PD to produce unstable feedback. The Discussion section includes more information on the motivation of this model structure and its agreement with previous movement studies.

To summarize, this candidate model includes four key changes to the model of Shadmehr and Krakauer [14]:

- Delay compensation: The model in [14] includes a single Kalman filter that receives non-delayed measurements, which does not address how an internal model extrapolates delayed measurements to produce non-delayed states. However, inclusion of this process is critical for capturing feedback instability.
- 2) Efferent copy of control input: The "known" control input is often considered to be captured by the efferent copy of the control input. However, this efferent copy represents the implemented input rather than the theoretically calculated input. The efferent copy provides additional information for delay compensation and is included here as a "measurement" for the Kalman filters.
- 3) Separates open-loop and feedback control: Delay compensation uses internal models to implement feedback with estimates of the non-delayed states. However, a non-feedback component executes without delay, requiring explicit inclusion of feedforward and feedback components.
- 4) Gating model: This addition represents the key dysfunction in PD. Excessive basal ganglia inhibition of the thalamus decreases rate-coded signals that normally facilitate movement in healthy motor control.

Significantly, this model approximately reduces to the Shadmehr and Krakauer [14] model when assuming perfect delay compensation and healthy gating. The explicit separation of open-loop and feedback control produces the same control inputs as a standard stochastic optimal feedback controller if the internal model matches the actual dynamics. These factors help to motivate the overall model structure because it inherently captures movement characteristics shown in [14] and other similar models based on optimal feedback control.

## A. Model

1) Dynamics: Simulations of a single degree-of-freedom (SDOF) joint model demonstrate the characteristics of the candidate motor control model. The equations of motion include joint inertia J, damping G, and stiffness K with angle  $\theta$ , muscular torque f, and external torque  $f_e$ . The implemented control input  $u_m$  represents muscle activation as a second-order low-pass filter with intermediate state g and time constants  $\tau_1$  and  $\tau_2$ :

$$J\ddot{\theta} + G\dot{\theta} + K\theta = f + f_e$$

$$\tau_2 \dot{f} + f = g$$

$$\tau_1 \dot{g} + g = u_m.$$
(1)

The implemented control input  $u_m$  includes the input calculated via feedback control  $u_{FB}$  and open-loop control  $u_{OL}$  along with the disturbance  $u_d$ :

$$u_m = b(u_{\text{OL}} + u_{\text{FB}} + u_d) \tag{2}$$

The gate parameter b blocks inputs for undesired tasks (b = 0) and facilitates inputs for desired tasks (b = 1). The control system treats  $u_d$  as a state: this setup allows the controller to overcome variations in the implemented control input, as observed in saccades [31].

The control system computes an input u using methods from optimal control theory. First, write the dynamics in standard

linear form:

$$\dot{x} = Ax + Bu \tag{3}$$

The known control input is

$$u = b(u_{\rm OL} + u_{\rm FB}). \tag{4}$$

Augment the state with the desired position  $\theta^*$ :

Approximating the dynamics over the small sample interval  $\Delta t$  enables discrete control design:

$$A_k \approx I + A\Delta t$$

$$B_k \approx \Delta t A_k B. \tag{6}$$

The dynamics may also include linear process noise  $\xi_k \sim \mathcal{N}(0, \Omega^{\xi})$ :

$$x_{k+1} = A_k x_k + B_k u_k + \xi_k \tag{7}$$

The noise terms allow the estimator to track states with uncertain dynamics, like  $f_e$  and  $u_d$ . Altogether, writing the dynamics in this standard linear form enables calculation of estimator and controller gains using LQG equations.

2) Bayesian Estimator: A Kalman filter estimates the full state from a partial-state measurement with noise  $\sigma_k \sim \mathcal{N}(0, \Omega^{\sigma})$ :

$$y_k = Hx_k + Du_k + \sigma_k. (8)$$

Assume muscle spindles measure  $\theta$  and  $\dot{\theta}$  via the muscle stretch and stretch rate while Golgi tendon organs measure torque f via muscle force [32]. The measurement also includes the efferent copy of the implemented control input  $u_m$ . Therefore, the observation matrices are

$$H = \begin{bmatrix} 1 & 0 & 0 & 0 & 0 & 0 & 0 \\ 0 & 1 & 0 & 0 & 0 & 0 & 0 \\ 0 & 0 & 1 & 0 & 0 & 0 & 0 \\ 0 & 0 & 0 & 0 & 0 & b & 0 \end{bmatrix}$$

$$D = \begin{bmatrix} 0 & 0 & 0 & b \end{bmatrix}^{\mathsf{T}}. \tag{9}$$

A Kalman filter creates a state estimate  $\hat{x}_k$  using fixed gains at each time step  $K_k$ :

$$\hat{x}_{k+1} = A_k \hat{x}_k + B_k u_k + K_k (y_k - H \hat{x}_k - D u_k) + \eta_k$$
 (10)

where  $\eta_k \sim \mathcal{N}(0, \Omega^{\eta})$  allows noise to be included in the estimator. A forward pass in time calculates the optimal estimator gains  $K_k$  given known initial state estimate  $\hat{x}_1$  with known covariance  $P_1$ :

$$K_k = A_k P_k H^{\top} (H P_k H^{\top} + \Omega^{\omega})^{-1}$$
  

$$P_{k+1} = \Omega^{\xi} + \Omega^{\eta} + (A_k - K_k H) P_k A_k^{\top}.$$
 (11)

3) Forward Model: The previously calculated state estimate represents the state at  $k-n_{\rm del}$ , where  $n_{\rm del}$  is number of time steps of the delay in the loop due to transmission time of signals to and from the CNS. A forward model overcomes this feedback delay to obtain a state estimate at the current time step. Another Kalman filter implements this component, operating in the same way as the previous filter but with the only "measurement" being the efferent copy of the control input. Thus,  $H = \begin{bmatrix} 0 & 0 & 0 & 0 & 0 & 0 \end{bmatrix}$  and D = b in the forward model filter. The forward model runs through  $n_{\rm del}$  iterations at every time step to obtain the state estimate at the current time step given the state estimate at  $k-n_{\rm del}$  and  $u_m$  from  $k-n_{\rm del}$  to k-1.

4) Controller: Human motor control demonstrates elements of both open-loop and closed-loop control. Some controller structures capture both of these elements implicitly—for example, a typical stochastic optimal control (SOC) system creates inputs that blend predictive and feedback components. However, the presented candidate model separates the controller contributions explicitly by including a model-based feedback component and an open-loop component. This structure allows the internal model of the feedback controller to include the open-loop input trajectory, providing more information to optimize feedback inputs. Furthermore, this structure better captures how the closed-loop response will change when the feedback controller has incorrect information about the open-loop controller, as in this PD model. Recent work by Berret et. al [18] demonstrates the importance of explicitly separating open-loop and feedback components to capture certain behaviors, labeling such systems as "stochastic optimal feedforward-feedback control" (SFFC). The net effect is very similar to SOC for many situations, but SFFC provides insight when the relative contributions and calculations for predetermined open-loop inputs and feedback inputs are important.

Both controllers apply optimal control theory with the classical quadratic form for the cost function:

$$Cost = \sum_{k=1}^{N} (x_k^{\top} Q_k x_k + u_k^{\top} R_k u_k)$$
 (12)

where  $Q_k$  and  $R_k$  may vary with time. The effort weighting matrix  $R_k$  is a scalar since the model includes only one input. The matrix  $Q_k$  captures the state-dependent task goals. This study simulates tasks to achieve or maintain a target position  $\theta^*$ , requiring minimization of  $(\theta - \theta^*)^2$ . The corresponding matrix is

$$Q_k = \begin{bmatrix} 1 & 0 & 0 & 0 & 0 & 0 & -1 \end{bmatrix}^{\mathsf{T}} \begin{bmatrix} 1 & 0 & 0 & 0 & 0 & 0 & -1 \end{bmatrix}.$$
(13)

For a rest task, this  $Q_k$  value holds for all k. For a reaching task, the feedback controller implements  $Q_k = 0$  when  $k < N_{\rm reach}$  to capture that the state is only required to reach the target at and after the target reaching time. The  $Q_k$  value holds for all k even for reaching for the open-loop controller. This format produces reaches that more closely resemble previously recorded wrist reaching in healthy and PD states, likely due to the stiffness-dominated dynamics of the wrist model. Note that this cost function form is used for mathematical convenience and quadratic cost functions do not accurately capture some

aspects of human motor control [12]. For example, optimizing movement duration using a squared force energy term implies the acceptance of excessively long durations for small rewards. In contrast, an empirically determined function for energetic cost does have a global minimum that rejects long movements for small rewards. However, the quadratic form is sufficient to evaluate the ability of the candidate model structure to capture tremor in PD because the qualitative behavior stems from the existence of model-based feedback. The intricacies of the feedback gains might affect higher-order behavior but retain the key qualitative features.

Both controllers determine the input  $u_k$  from the state estimate and controller gains  $L_k$ :

$$u_k = -L_k \hat{x}_k \tag{14}$$

Known final value  $S_N = Q_N$  enables calculation of the optimal gains backward in time from final time step N:

$$L_{k} = \left(R_{k} + B_{k}^{\top} S_{k+1} B_{k}\right)^{-1} B_{k}^{\top} S_{k+1} A_{k}$$

$$S_{k} = Q_{k} + A_{k}^{\top} S_{k+1} (A_{k} - B_{k} L_{k}). \tag{15}$$

The open-loop controller gains and inputs are calculated before task execution using the initial state estimate and model of task dynamics. In other words, the gains produce all  $u_{OL}$  values based on the expected path and these values are known and available for the feedback controller. Receding horizon optimal control (RHOC) implements the feedback controller to capture the ability of human motor feedback to adapt in real time. Thus, the feedback gain  $L_k$  is calculated at each time step as the optimal initial gain matrix for an optimal gain trajectory from the current time step to  $N_{\rm RHOC}$  steps in the future. Significantly, the RHOC calculation includes the expected open-loop inputs in the system dynamics by augmenting the state: the additional state is always 1 and  $A_k(4, 8) = \frac{b}{\tau_1} u_{OL}$ at each time step. The addition of this trivial state means the internal model used to calculate optimal feedback gains includes information about how the open-loop input changes the dynamics. The augmented  $A_k$  matrix affects the optimal feedback gains through the  $L_k$  calculations. Therefore, feedback primarily addresses deviations from the expected motion to achieve task goals despite unknown disturbances.

5) Gate: The gate is motivated by the basal ganglia gating model whereby the basal ganglia effectively inhibits and facilitates undesired and desired movements, respectively. For healthy individuals, the gate value b = 0 for undesired movements and b = 1 for desired movements. Since simulations represent desired actions, the model used by the control system always has b = 1. However, this study characterizes PD by setting the implemented b < 1 to represent a decreased signal amplitude—the control system is unaware of this pathological change and implements control believing b = 1. This mismatch between internal model parameters and actual parameters can produce unstable feedback. Physiologically, a GABA-modulated multiplicative change in neural gain could implement this type of multiplicative gating effect [33]. This gain modulation may be shifted towards lower gains through the excessive inhibition of VLa in PD.

This study defines a PD parameter  $X_{PD}$  to better visualize the effect of PD on model simulations. This parameter ranges from 0 to 1 with 0 representing a healthy individual and 1 representing the highest possible level of PD pathology. Greater pathology means greater dopamine depletion, which reduces the gate value b in the presented model. This paper implements a straightforward relationship between  $X_{PD}$  and b:

$$b = 1 - X_{PD}.$$
 (16)

The actual relationship between disease progression and gate value is likely nonlinear and is subject to future research. Still, this linear relationship provides qualitative insight into how movement dysfunction may change during progression of PD.

#### B. Simulations

In the following simulations, model parameters represent wrist flexion-extension:  $J = 0.00276 \text{ Nms}^2/\text{rad}$ , G =0.03 Nms/rad, and K = 0.992 Nm/rad with muscle time constants  $\tau_1 = \tau_2 = 40$  ms [34]. The control input saturates at u = 2 to produce stable oscillations during unstable feedback. The discretization time step is  $\Delta t = 1$  ms and the measurement delay is  $t_{\text{del}} = 100 \text{ ms}$ . The nonzero process noise covariance matrix values used to calculate gains are  $\Omega^{\xi}(1,1) = 1.75 \times 10^{-7}, \ \Omega^{\xi}(2,2) = 8.53 \times 10^{-7}, \ \Omega^{\xi}(3,3) =$  $1.16 \times 10^{-7}$ ,  $\Omega^{\xi}(4,4) = 1.39 \times 10^{-7}$ ,  $\Omega^{\xi}(5,5) = 1.16 \times 10^{-7}$  $10^{-6}$ , and  $\Omega^{\xi}(6,6) = 1.39 \times 10^{-6}$ . Nonzero measurement noise covariance matrix values are  $\Omega^{\omega}(1, 1) = 1.75 \times 10^{-4}$ .  $\Omega^{\omega}(2,2) = 8.53 \times 10^{-4}, \ \Omega^{\omega}(3,3) = 1.16 \times 10^{-4}, \ \text{and}$  $\Omega^{\omega}(4,4) = 1.39 \times 10^{-4}$ . These values were selected based on average value changes per step of a typical reaching trajectory. All other noise and covariance terms are zero. For reaching simulations, gains were calculated using  $N_{\text{reach}} =$ 250,  $N_{\rm RHOC} = 500$ , and  $R_k = 5 \times 10^{-2}$ . For rest simulations,  $u_{\rm OL} = 0$ ,  $R_k = 1 \times 10^{-4}$ , and  $N_{\rm RHOC} = 500$ .

First, reaching and rest simulations with varying levels of  $X_{\rm PD}$  demonstrate the ability of the model to capture healthy movement and tremor in PD. Figure 3 presents these simulations for a healthy case ( $X_{\rm PD}=0$ ) and five PD cases with increasing levels of pathology. Rest simulations include a small perturbation to engage a controller response. Healthy parameters produce accurate reaching and maintain rest position. Rest tremor appears above some threshold  $X_{\rm PD}$  value, then decreases as  $X_{\rm PD}$  increases, at least for this set of parameters. Significantly, PD cases with rest tremor still accomplish the reaching task and appear to have longer reaching durations consistent with reduced motor vigor. Furthermore, these simulated reach traces appear remarkably similar to previously recorded PD wrist movements [35].

Figure 4 highlights the variability of rest tremor severity given PD severity. The figure presents the rest tremor amplitude and frequency for several sets of control gains across the range of possible disease parameters  $X_{\rm PD}$ . The only parameter changed in each gain set is  $R_k$ , ranging from about  $6 \times 10^{-5}$  to  $1 \times 10^{-3}$ . Higher values of  $R_k$  produce lower magnitudes of controller gains while lower  $R_k$  values produce higher gains. These different sets of gains demonstrate how different individuals might be affected differently by PD pathophysiology. Each datapoint represents a single simulation for that combination of control gains and disease parameter, with datapoints connected to provide visual clarity. Thus, the rest tremor simulations in Fig. 3 map onto Fig. 4 as six datapoints. Higher controller gains produce a large jump in tremor amplitude above a threshold  $X_{\rm PD}$  value,

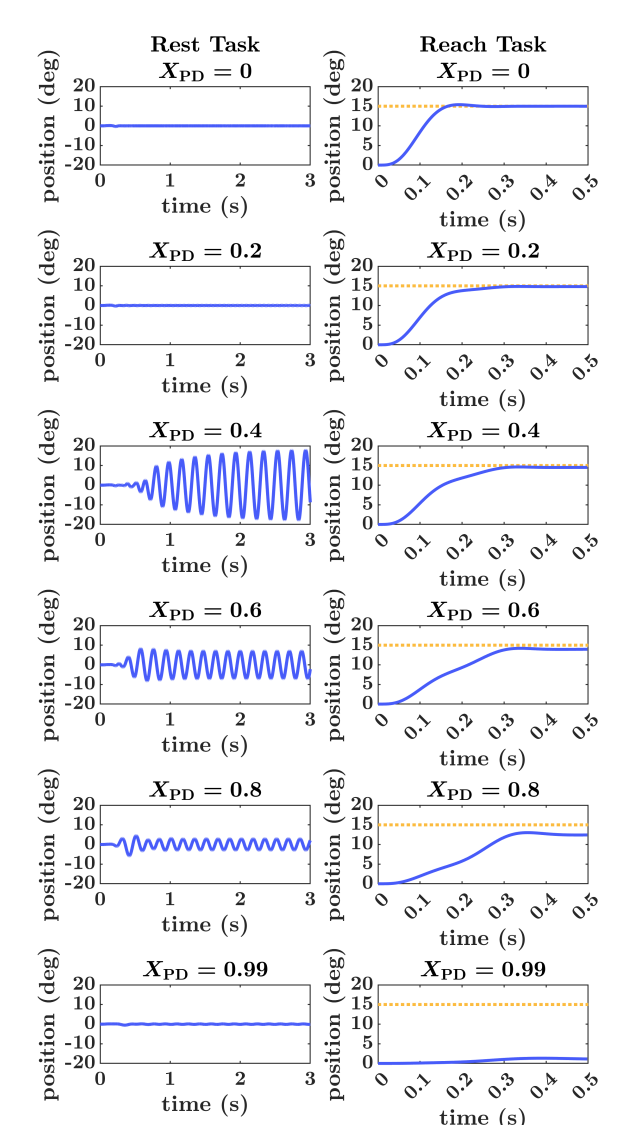


Fig. 3. Simulations of reaching and rest for varying disease parameter values. Reach target shown as dotted line.

here about 0.25. Then, increasing pathology decreases tremor amplitude and increases tremor frequency. In contrast, lower controller gains produce a more gradual tremor progression and a decreasing tremor frequency. Interestingly, all gain sets converge towards a single frequency as  $X_{PD}$  increases: in this case, about 6 Hz. Overall, these results indicate that tremor progression can vary among different individuals due to different inherent controller parameters. Furthermore, tremor expression can vary in an individual as controller gains change for different situations. Figure 4 also illustrates the fraction of time for which the controller input is saturated for each simulation. Saturation fraction does not change significantly across disease parameters for a given set of gains. Gain sets exhibiting the "increasing-frequency" characteristics have very high saturation fractions above about 0.95. Further simulations (not illustrated) investigated the effects of saturation amplitude and feedback delay magnitude. Higher saturation amplitudes produce higher tremor amplitudes without changing tremor frequency, similar to the effects of delay-induced unstable feedback [7]. Changing the delay magnitude changes the tremor amplitude (greater delay produces greater tremor) but

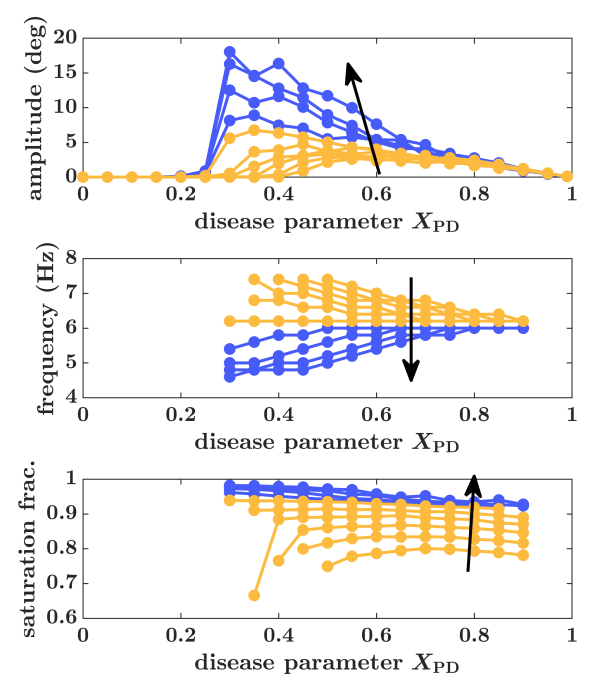


Fig. 4. Rest tremor amplitude, frequency, and controller saturation fraction for varying sets of feedback gains and disease parameters. Dark traces indicate parameter sets that have final tremor frequency values greater than initial values. Arrows point towards trends as the sets of feedback gains increase.

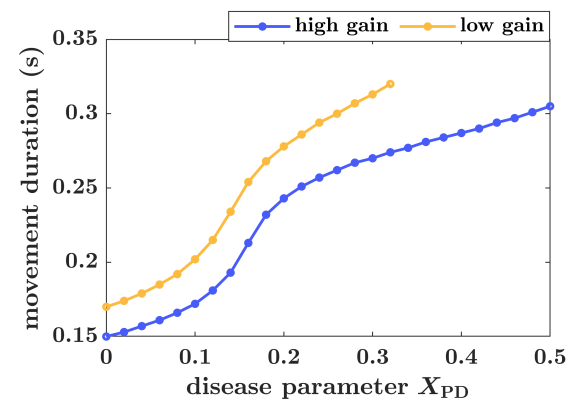


Fig. 5. Reaching movement duration for two sets of feedback gains with varying disease parameters.

also changes the frequency for which the different gain sets converge, with longer delays producing lower frequencies. For example, a 140 ms sensory delay produces tremor that converges towards 5 Hz as  $X_{\rm PD}$  increases. Future work will perform an in-depth parameter analysis to gain further insight into how key parameters affect system characteristics.

Reaching simulations in Fig. 3 hint at the candidate model's ability to capture both tremor and reduced vigor with a single disease parameter. Figure 5 verifies this observation by determining the movement duration as the 5% settling time for reaches: higher disease parameters reduce motor vigor (i.e., increase movement duration). The model can also recreate results similar to the study by Mazzoni et al. [11] that demonstrates a reduced willingness of PD patients to move fast. For example, the peak velocities from the displayed reaching simulations for  $X_{\rm PD}=0$  and  $X_{\rm PD}=0.2$  are 2.78 rad/s and 2.34 rad/s, respectively. Consider the case where the target peak reach velocity is 3 rad/s and the CNS adapts by

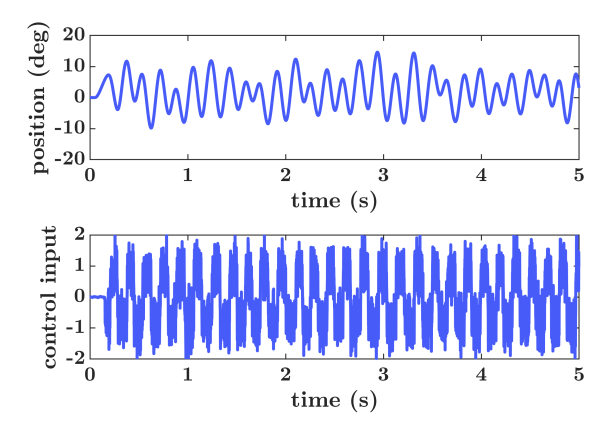


Fig. 6. Inclusion of control input multiplicative noise produces time-varying tremor amplitude.

decreasing  $R_k$  by 5% of its original value after each failed trial (therefore, increasing gains to move faster on the subsequent trial). The PD case (with  $X_{\rm PD}=0.2$ ) takes 17 iterations for a trial to reach the target velocity while the healthy case ( $X_{\rm PD}=0$ ) takes 8 trials to produce a movement with the target velocity. Thus, it takes this theoretical PD patient 9 additional trials to reach the target velocity.

The simulated model aims to capture the qualitative characteristics of PD movement dysfunction. Multiplicative noise is a well-established factor in human motor control but is not included in this initial model. The optimal control equations and Kalman filter equations are only optimal for linear noise and the inclusion of multiple filters and controller calculations makes the model incompatible with previous SOC derivations for multiplicative noise [36]. However, simulations with multiplicative control input noise still provide insight into how this noise might affect the system. Reaching simulations produce qualitatively similar results as without noise (but with greater variation). However, as illustrated in Fig. 6, multiplicative noise produces time-varying tremor amplitude that more closely resembles tremor observed in patient recordings. This result helps to illustrate how a single high-level control system parameter can produce the complex limb oscillations observed in PD patients.

Finally, this model structure is motivated by PD but may provide insight into other movement dysfunctions. A brief example is provided here for cerebellum dysfunction. Consider the saccades study by Xu-Wilson et al. [31] where saccade targets were repeated to effectively decrease motivation. Simulations in Fig. 7 recreate these results with the presented wrist model adjusted to have control similar to saccades. Set  $\Omega^{\omega}$  values to be very high for  $\theta$ ,  $\dot{\theta}$ , and f since saccades suppress sensory feedback. The decreased motivation to move is captured here by setting b = 0.7. In other words, reduced motivation decreases task reward enough to cause the basal ganglia gate to open only partially. In healthy subjects, unexpectedly low initial control inputs are overcome by feedback of the implemented control values  $u_m$ . However, the forward model in cerebellar patients is dysfunctional, implemented here by removing  $u_{FB}$  altogether since now there is no reliable feedback information. Figure 7 shows model simulations agree with the observed saccades for healthy and cerebellar patients from [31]: cerebellar patients are unable to overcome the low initial control inputs and fall short of the target. The treatment

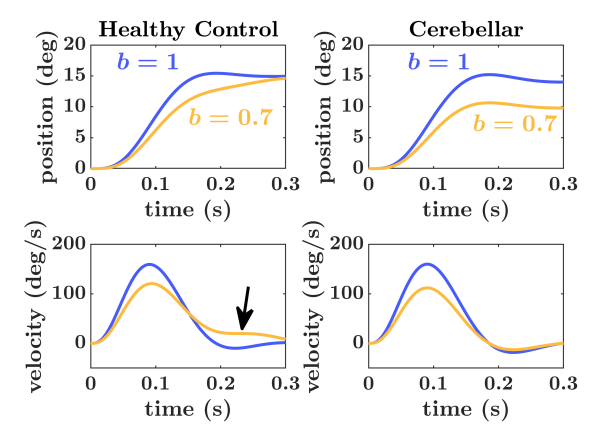


Fig. 7. Reaching with suppressed sensory feedback and decreased motivation for healthy and cerebellar cases.

of the implemented control input as a measurement in the forward model Kalman filter is a key component for capturing this behavior. Future work will aim to further analyze how this type of model structure could provide insight into PD and other sources of movement dysfunction.

#### IV. DISCUSSION

To start, the motivation of the model structure is based on the physiological underpinnings of the gating model of basal ganglia control of the thalamus. Tonic inhibition suppress thalamic output to the cortex while disinhibition allows thalamic excitation of the cortex. Excessive inhibition in PD decreases thalamus firing rates in the "disinhibited" state relative to healthy firing rates. This signal may act as a nonlinear "on/off" gain factor for activation in the cortex. The shift in firing rate in PD causes the system to operate in the transition region of the on/off gate, decreasing the level of the control input. Of course, this example gating mechanism is very speculative and represents only one of many potential mechanisms for unstable feedback through decreased signals. The control-system roles and connectivity of brain regions implies that this type of decrease in control signal would occur in the cortex via the thalamus or directly in the thalamus these facts informed model development. However, the model does not explicitly require this function to happen in any specific region. Overall, the key physiological motivation for this model is the fact that excessive inhibition in PD would decrease the amplitude of rate-coded signals. The rest of the model structure is informed by previous clinical studies regarding theory for roles of brain regions, previous evidence that the brain uses internal models to overcome sensory delays, and previous evidence that unstable feedback could produce tremor.

The candidate model aligns well with existing knowledge about parkinsonian tremor. First, the theory does not preclude the dimmer-switch hypothesis since the observed neural activity that motivates the dimmer-switch hypothesis may represent lower-level implementation of higher-level motor control [9]. In other words, the basal ganglia triggering tremor is analogous to initiating a motor program to complete a task while CTC oscillation represents the oscillatory state in feedback control. The basal ganglia and CTC circuit still trigger and drive tremor, respectively, but there is more insight into the source of dysfunction. The model also captures the potential

mechanisms for PD treatment effectiveness. Dopaminergic medications raise dopamine levels to directly increase the gate value by reducing net inhibition of VLa. Some patients have dopamine-resistant tremor, which could be the result of effectively decreasing  $X_{\rm PD}$  in Fig. 4, but not enough to get past the threshold that produces tremor. In addition, it is possible other mechanisms may make it appear as if dopamine treatment is ineffective [37]. DBS targeting the basal ganglia also reduces net inhibition by disrupting inhibition stemming from GPi or the subthalamic nucleus (STN) [38], [39]. DBS of VLp disrupts the feedback loop, disrupting the instability that causes tremor but requiring the motor system to rely on open-loop control or implement alternative mechanisms of feedback control [40]. One possibility is the state estimate skips forward estimation in the cerebellum: the PPC processes delayed measurements and directly sends a delayed state estimate to the motor cortex. This setup still allows movements to adapt, but less rapidly. This setup may also produce similar movements as cerebellar patients, which may be investigated in future studies.

In addition to DBS treatment, a recent study evaluated the effect of electrical stimulation of thalamic and basal ganglia regions at different frequencies (other than the > 100 Hz frequencies of DBS) [41]. Stimulation activates all synapses at the stimulation location, so firing rates increase for regions with relatively more excitatory synapses (thalamic regions) and decrease for regions with relatively more inhibitory synapses (basal ganglia regions). Therefore, stimulation of either region has an excitatory effect on the thalamus and likely increases movement (though whether movement was produced was not reported). Overall, thalamic output depends on the net effect of inhibitory and excitatory contributions. Thus, increased inhibition will decrease firing rate. Both regions experience reduced firing at high stimulation frequencies (> 100 Hz) due to synaptic fatigue, which is consistent with the effectiveness of DBS as described previously.

Previous studies on how tremor changes in different context provides further insight into the efficacy of the candidate model. First, fixing the affected limb in a cast reduces or eliminates tremor EMG activity [42]. This reduced EMG activity shows that tremor is not driven by purely central drivers and feedback must play a role (otherwise, the central oscillator would continue to excite muscles at the same level even if the limb cannot move). In the context of the model, the inability to amplify the feedback signals prevents unstable feedback control and eliminates tremorous activation. Other studies indicate a potential modulatory (but not driving) role of peripheral feedback, with one source of evidence being that added mass does not change tremor frequency [43]. Significantly, model simulations with an order-of-magnitude increase in inertia produce less than a 0.5 Hz shift in tremor frequency. In addition, studies show the long-latency strech reflex (LLSR) includes information about internal models and likely includes cortical processing [44], [45], [46]. Thus, the LLSR might implement an equivalent of the feedback component of the control framework in this paper. This idea highlights how peripheral feedback through the CNS that becomes unstable could produce tremor.

Next, increased stress and cognitive load both increase tremor amplitude [47], [48]. Stress increases movement speed,

which may represent an increase in controller gains [49], [50]. This change could be represented through a decrease in  $R_k$  in the model to produce a higher magnitude of control inputs for both the open-loop and feedback components. Thus, stress would increase tremor amplitude as seen in the higher gain cases in Fig. 4. With this interpretation, stress should also decrease tremor frequency. However, [47] did not show a significant change in frequency. Perhaps stress also affects the level of dysfunctional gating to increase amplitude while counteracting the change in frequency. This discrepancy requires further investigation in future work. Cognitive load decreases movement accuracy, which may represent decreased state estimation accuracy due to reduced cognitive resources [51]. Increased measurement noise could represent this change, which skews feedback to weigh internal models more heavily, increasing tremor amplitude since the internal model does not accurately represent the actual dynamics. The increased cerebral integration observed during cognitive load may reflect this increased reliance on the internal model since multiple brain regions are sharing and collaborating with the same internal model [3], [48].

Previous clinical studies on the effect of disease progression on tremor produce mixed conclusions. One longitudinal study on PD tremor frequency found that frequency decreases by approximately 0.1 Hz per year, on average [52]. However, a significant change in frequency was only observed in about half of the patients, with 30% of those patients exhibiting a frequency increase rather than decrease. Unfortunately, this longitudinal study did not measure tremor amplitude or severity. Another study evaluating patients with asymmetrical tremor symptoms found tremor disability scores increase over time, on average [53]. A review on DBS effectiveness over time found that tremor severity increased the least among all symptoms and decreased in a quarter of studies [54]. A study on the effectiveness of levodopa over time found tremor decreased on average, especially in the non-tremor subtype but also in tremor-dominant patients [55]. Altogether, this variation of tremor amplitude and frequency progression across patients and studies is not surprising in the context of Fig. 4. Different patients will have different effective controller parameters, which affects how tremor will change due to increased pathology.

Continuing this discussion, it is also known that some tremor-dominant patients lose their tremor as the disease progresses [56]. Another study observed high variation in tremor amplitude for tremor-dominant patients, but low variation for high-rigidity patients [57]. In addition, high-rigidity patients with no visible tremor still had measurable tremor. The loss of tremor for high disease parameters explains the existence of tremor and non-tremor phenotypes and the transition of some patients from the tremor to non-tremor phenotype. The tremor-dominant phenotype is associated with less severe symptoms and less depletion of dopaminergic cells [58]. Thus, non-tremor patients have high disease parameters that are past the tremor-producing region. Tremor-dominant patients that lose tremor have dopaminergic cell depletion that advances them to the non-tremor portion of Fig. 4.

The candidate model demonstrates that tremor can extend from the same pathology as bradykinesia (through basal ganglia dopamine depletion). Decreased dopamine increases thalamic inhibition that decreases the gate value to produce slow volitional movements and unstable feedback at rest. Since the basal ganglia is also believed to define the costs and rewards for a task [14], decreased dopamine could also reduce the represented value of the task to further decrease motor vigor [12]. Rigidity—the other key PD motor symptom could be a response to instability, similar to the increased stiffness and damping from co-contraction observed in healthy individuals in uncertain environments [59], [60]. Rigidity could also play a role in modifying tremor as disease progresses [57]. The general inhibition of movement for severe PD could be a combination of the effects of reduced vigor and increased rigidity. Finally, while this paper focuses on movement dysfunction of upper limbs, the model could provide insight into gait dysfunction in PD. Gait is predominantly feedforward-controlled due to the longer sensory delays as compared to the upper-limbs [61]. Consequently, there is less opportunity for feedback to overcome the decreased amplitudes of pathologically gated open-loop input. This effect could appear as characteristic PD gait symptoms like shuffling or freezing of gait as the legs do not reach the full scale of their desired trajectory [62]. Future work will investigate the potential for this type of model to characterize PD gait symptoms.

In addition to PD, the candidate model captures movement characteristics of healthy individuals as well as other movement dysfunctions, particularly since it largely follows the form of Shadmehr and Krakauer's model [14]. Cerebellar movements that cannot overcome decreased motor gains represent a key feature the updated model captures which was not explicitly captured previously [31]. Figure 7 illustrates how the model captures the inability of cerebellar patients to incorporate the descending control input into a forward model to overcome unexpectedly low inputs. Extensions of the candidate model could capture other cerebellar effects like essential tremor, which could be the result of faulty delay compensation in the cerebellum [6].

Future studies could further advance these control framework models of human motor control to improve our understanding of qualitative roles of brain regions. In addition, longitudinal studies measuring tremor amplitude and frequency along with the severity of bradykinesia and rigidity can provide insight into disease progression and support for the proposed mechanism of tremor generation. Future research can also use the predicted tremor progression trends to improve diagnosis and treatment. Analysis of tremor frequency over time could indicate the level of disease progression and identify when a patient is approaching the rigid phenotype. Alternative treatments could exploit knowledge of system dynamics to develop mechanical or neurological rehabilitation approaches to improve symptoms. For example, patients can reduce tremor amplitude through volitional suppression, which is associated with decreased muscular activation [63]. This volitional suppression could be the result of a voluntary change in the control parameters (e.g., reducing the value of maintaining target position to decrease gains). Knowledge of the expected control system structure and dysfunction could identify cues to train patients to mitigate their symptoms. One possibility is improving bradykinesia by training patients to imagine reaching for something that is much more valuable

than the actual item, thereby improving motor vigor. Even simply making patients aware of how dysfunction affects their motor control could enable volitional compensation of symptoms.

The model can provide insight into new pharmaceutical treatments that aim to increase the gate value or otherwise improve closed-loop stability. One possibility is the use of drugs that increase motor impulsivity, which could correspond to a more easily opened gate. Indeed, levodopa is associated with increased impulsivity and dyskinesia when treating PD patients [64]. Those side effects could represent an overshoot of the desired effect of fully opening the gate more easily. Research shows that serotonin is also affected by PD: interestingly, serotonin depletion increases impulsive movements and is linked to tremor-dominant PD [65], [66]. These two observations point towards the possibility that serotonin works in concert with dopamine to characterize the costs and rewards for a task. Treatment approaches that modulate serotonin levels—even decreasing serotonin—could benefit patients by restoring the correct ratio and could depend on where the patient is in the disease progression life cycle.

Finally, while this study provides promising results towards improved understanding of PD, it is important to highlight that this initial theory development requires much further analysis through future studies. This paper develops a low-order model motivated by qualitative roles and connectivity. The CNS is extremely complex and such a low-order model cannot capture all features of human motor control. Furthermore, while simulations demonstrate clinically observed characteristics, other models or mechanisms could also capture the same features. Future work should identify movement studies that would show clear differences in recorded movements consistent with the proposed model as opposed to other potential candidate models for human motor control. These types of movement studies could also identify potential diagnosis strategies that exploit predicted differences in PD and healthy movement.

## V. CONCLUSION

In summary, augmenting a computational neuroanatomy framework to include a mechanism of unstable feedback in PD captures healthy control, parkinsonian tremor, and other mechanisms of movement dysfunction. Key additions to the control system framework include the basal ganglia gating model and the treatment the efferent copy of the control input as a measurement, similar to proprioceptive feedback. The model captures excessive thalamic inhibition in PD as a reduced gate value since inhibition is expected to reduce rate-coded signal amplitude. This reduced gate value can produce unstable feedback since the internal model is unaware of the pathological change. Significantly, the proposed mechanism of tremor generation allows dopamine depletion to cause all of the primary motor symptoms in PD: rigidity, bradykinesia, and tremor. Tremor severity and frequency vary over the life cycle of disease progression in a way that matches the inconsistent results of longitudinal studies. Simulations show the disappearance of tremor for severe disease cases, representing the non-tremor PD phenotype and the disappearance of tremor in some patients. Altogether, the proposed mechanism of PD tremor generation along with the computational neuroanatomy framework provide insight into treatment effectiveness, disease progression, and pathways towards improved understanding of human motor control.

#### **ACKNOWLEDGMENT**

The authors would like to thank Helen J. Huang for the discussions that helped inspire this work.

### REFERENCES

- D. W. Franklin and D. M. Wolpert, "Computational mechanisms of sensorimotor control," *Neuron*, vol. 72, no. 3, pp. 425–442, Nov. 2011.
- [2] S. H. Scott, "A functional taxonomy of bottom-up sensory feedback processing for motor actions," *Trends Neurosciences*, vol. 39, no. 8, pp. 512–526, Aug. 2016.
- [3] R. S. Maeda, T. Cluff, P. L. Gribble, and J. A. Pruszynski, "Feedforward and feedback control share an internal model of the arm's dynamics," *J. Neurosci.*, vol. 38, no. 49, pp. 10505–10514, Dec. 2018.
- [4] J. A. Pruszynski and S. H. Scott, "Optimal feedback control and the long-latency stretch response," *Exp. Brain Res.*, vol. 218, no. 3, pp. 341–359, May 2012.
- [5] M. Desmurget and S. Grafton, "Forward modeling allows feedback control for fast reaching movements," *Trends Cogn. Sci.*, vol. 4, no. 11, pp. 423–431, Nov. 2000.
- [6] F. Crevecoeur and M. Gevers, "Filtering compensation for delays and prediction errors during sensorimotor control," *Neural Comput.*, vol. 31, no. 4, pp. 738–764, Apr. 2019.
- [7] V. V. Shah, S. Goyal, and H. J. Palanthandalam-Madapusi, "Clinical facts along with a feedback control perspective suggest that increased response time might be the cause of parkinsonian rest tremor," J. Comput. Nonlinear Dyn., vol. 12, no. 1, Jan. 2017, Art. no. 011007.
- [8] C. R. Kelley and J. L. Kauffman, "Optimal control perspective on Parkinson's disease: Increased delay between state estimator and controller produces tremor," *IEEE Trans. Neural Syst. Rehabil. Eng.*, vol. 28, no. 10, pp. 2144–2152, Oct. 2020.
- [9] R. C. Helmich, M. Hallett, G. Deuschl, I. Toni, and B. R. Bloem, "Cerebral causes and consequences of Parkinsonian resting tremor: A tale of two circuits?" *Brain*, vol. 135, no. 11, pp. 3206–3226, Nov. 2012.
- [10] R. L. Albin, A. B. Young, and J. B. Penney, "The functional anatomy of basal ganglia disorders," *Trends Neurosciences*, vol. 12, no. 10, pp. 366–375, Jan. 1989.
- [11] P. Mazzoni, A. Hristova, and J. W. Krakauer, "Why don't we move faster? Parkinson's disease, movement vigor, and implicit motivation," *J. Neurosci.*, vol. 27, no. 27, pp. 7105–7116, Jul. 2007.
- [12] R. Shadmehr, H. J. Huang, and A. A. Ahmed, "A representation of effort in decision-making and motor control," *Current Biol.*, vol. 26, no. 14, pp. 1929–1934, Jul. 2016.
- [13] R. C. Helmich, I. Toni, G. Deuschl, and B. R. Bloem, "The pathophysiology of essential tremor and Parkinson's tremor," *Curr. Neurol. Neurosci. Rep.*, vol. 13, no. 9, p. 378, 2013.
- [14] R. Shadmehr and J. W. Krakauer, "A computational neuroanatomy for motor control," *Exp. Brain Res.*, vol. 185, no. 3, pp. 359–381, 2008.
- [15] E. Todorov and M. I. Jordan, "Optimal feedback control as a theory of motor coordination," *Nature Neurosci.*, vol. 5, no. 11, pp. 1226–1235, Nov. 2002.
- [16] S. Haar and O. Donchin, "A revised computational neuroanatomy for motor control," *J. Cogn. Neurosci.*, vol. 32, no. 10, pp. 1823–1836, Oct. 2020.
- [17] W. P. Medendorp and T. Heed, "State estimation in posterior parietal cortex: Distinct poles of environmental and bodily states," *Prog. Neurobiol.*, vol. 183, Dec. 2019, Art. no. 101691.
- [18] B. Berret, A. Conessa, N. Schweighofer, and E. Burdet, "Stochastic optimal feedforward-feedback control determines timing and variability of arm movements with or without vision," *PLOS Comput. Biol.*, vol. 17, no. 6, Jun. 2021, Art. no. e1009047.
- [19] C. Bosch-Bouju, B. I. Hyland, and L. C. Parr-Brownlie, "Motor thalamus integration of cortical, cerebellar and basal ganglia information: Implications for normal and parkinsonian conditions," *Frontiers Comput. Neurosci.*, vol. 7, p. 163, Nov. 2013.
- [20] O. Hikosaka, "GABAergic output of the basal ganglia," Prog. Brain Res., vol. 160, pp. 209–226, Jan. 2007.
- [21] A. Tewari, R. Jog, and M. S. Jog, "The striatum and subthalamic nucleus as independent and collaborative structures in motor control," *Frontiers Syst. Neurosci.*, vol. 10, p. 17, Mar. 2016.

- [22] H. J. Palanthandalam-Madapusi and S. Goyal, "Is parkinsonian tremor a limit cycle?" *J. Mech. Med. Biol.*, vol. 11, no. 5, pp. 1017–1023, Dec. 2011.
- [23] V. V. Shah, S. Goyal, and H. J. Palanthandalam-Madapusi, "A possible explanation of how high-frequency deep brain stimulation suppresses low-frequency tremors in Parkinson's disease," *IEEE Trans. Neural Syst. Rehabil. Eng.*, vol. 25, no. 12, pp. 2498–2508, Dec. 2017.
- [24] F. S. Chance, L. F. Abbott, and A. D. Reyes, "Gain modulation from background synaptic input," *Neuron*, vol. 35, no. 4, pp. 773–782, Aug. 2002.
- [25] S. J. Mitchell and R. A. Silver, "Shunting inhibition modulates neuronal gain during synaptic excitation," *Neuron*, vol. 38, no. 3, pp. 433–445, May 2003.
- [26] A. Semyanov, M. C. Walker, D. M. Kullmann, and R. A. Silver, "Tonically active GABAA receptors: Modulating gain and maintaining the tone," *Trends Neurosciences*, vol. 27, no. 5, pp. 262–269, May 2004.
- [27] H. Blumenfeld, Neuroanatomy Through Clinical Cases. Sunderland, MA, USA: Sinauer Associates, 2010.
- [28] J. A. Pruszynski, I. Kurtzer, J. Y. Nashed, M. Omrani, B. Brouwer, and S. H. Scott, "Primary motor cortex underlies multi-joint integration for fast feedback control," *Nature*, vol. 478, no. 7369, pp. 387–390, Oct. 2011.
- [29] M. Farrant and Z. Nusser, "Variations on an inhibitory theme: Phasic and tonic activation of GABAA receptors," *Nature Rev. Neurosci.*, vol. 6, no. 3, pp. 215–229, Mar. 2005.
- [30] A. N. Burkitt, "A review of the integrate-and-fire neuron model: I. Homogeneous synaptic input," *Biol. Cybern.*, vol. 95, no. 1, pp. 1–19, Jul. 2006.
- [31] M. Xu-Wilson, H. Chen-Harris, D. S. Zee, and R. Shadmehr, "Cerebellar contributions to adaptive control of saccades in humans," *J. Neurosci.*, vol. 29, no. 41, pp. 12930–12939, Oct. 2009.
- [32] E. Burdet, D. W. Franklin, and T. E. Milner, Human Robotics: Neuromechanics and Motor Control. Cambridge, MA, USA: MIT Press, 2013
- [33] K. A. Ferguson and J. A. Cardin, "Mechanisms underlying gain modulation in the cortex," *Nature Rev. Neurosci.*, vol. 21, no. 2, pp. 80–92, Eab. 2020.
- [34] A. W. Peaden and S. K. Charles, "Dynamics of wrist and forearm rotations," J. Biomechanics, vol. 47, no. 11, pp. 2779–2785, Aug. 2014.
- [35] A. Berardelli, J. P. Dick, J. C. Rothwell, B. L. Day, and C. D. Marsden, "Scaling of the size of the first agonist EMG burst during rapid wrist movements in patients with Parkinson's disease," *J. Neurol., Neuro*surgery Psychiatry, vol. 49, no. 11, pp. 1273–1279, Nov. 1986.
- [36] E. Todorov, "Stochastic optimal control and estimation methods adapted to the noise characteristics of the sensorimotor system," *Neural Comput.*, vol. 17, no. 5, pp. 1084–1108, May 2005.
- [37] J. Nonnekes, M. H. M. Timmer, N. M. de Vries, O. Rascol, R. C. Helmich, and B. R. Bloem, "Unmasking levodopa resistance in Parkinson's disease," *Movement Disorders*, vol. 31, no. 11, pp. 1602–1609, Nov. 2016.
- [38] S. Chiken and A. Nambu, "Mechanism of deep brain stimulation: Inhibition, excitation, or disruption?" *Neuroscientist*, vol. 22, no. 3, pp. 313–322, Jun. 2016.
- [39] J. K. Wong et al., "STN vs. GPi deep brain stimulation for tremor suppression in Parkinson disease: A systematic review and meta-analysis," *Parkinsonism Rel. Disorders*, vol. 58, pp. 56–62, Jan. 2019.
- [40] L. Milosevic, S. K. Kalia, M. Hodaie, A. M. Lozano, M. R. Popovic, and W. D. Hutchison, "Physiological mechanisms of thalamic ventral intermediate nucleus stimulation for tremor suppression," *Brain*, vol. 141, no. 7, pp. 2142–2155, Jul. 2018.
- [41] L. Milosevic et al., "A theoretical framework for the site-specific and frequency-dependent neuronal effects of deep brain stimulation," *Brain Stimulation*, vol. 14, no. 4, pp. 807–821, Jul. 2021.
- [42] J. A. Burne, "Reflex origin of parkinsonian tremor," Experim. Neurol., vol. 97, no. 2, pp. 327–339, Aug. 1987.
- [43] M. F. Dirkx and M. Bologna, "The pathophysiology of Parkinson's disease tremor," J. Neurol. Sci., vol. 435, Apr. 2022, Art. no. 120196.
- [44] I. L. Kurtzer, J. A. Pruszynski, and S. H. Scott, "Long-latency reflexes of the human arm reflect an internal model of limb dynamics," *Current Biol.*, vol. 18, no. 6, pp. 449–453, Mar. 2008.
- [45] F. Crevecoeur and S. H. Scott, "Priors engaged in long-latency responses to mechanical perturbations suggest a rapid update in state estimation," *PLoS Comput. Biol.*, vol. 9, no. 8, Aug. 2013, Art. no. e1003177.

- [46] F. Crevecoeur and I. Kurtzer, "Long-latency reflexes for inter-effector coordination reflect a continuous state feedback controller," *J. Neuro*physiol., vol. 120, no. 5, pp. 2466–2483, Nov. 2018.
- [47] H. Zach, M. F. Dirkx, J. W. Pasman, B. R. Bloem, and R. C. Helmich, "Cognitive stress reduces the effect of levodopa on Parkinson's resting tremor," CNS Neurosci. Therapeutics, vol. 23, no. 3, pp. 209–215, Mar. 2017.
- [48] M. F. Dirkx, J. M. Shine, and R. C. Helmich, "Integrative brain states facilitate the expression of Parkinson's tremor," *Movement Disorders*, vol. 38, no. 9, pp. 1615–1624, Sep. 2023.
- [49] G. A. Metz, N. M. Jadavji, and L. K. Smith, "Modulation of motor function by stress: A novel concept of the effects of stress and corticosterone on behavior," *Eur. J. Neurosci.*, vol. 22, no. 5, pp. 1190–1200, Sep. 2005.
- [50] G. S. Shields, A. M. Rivers, M. M. Ramey, B. C. Trainor, and A. P. Yonelinas, "Mild acute stress improves response speed without impairing accuracy or interference control in two selective attention tasks: Implications for theories of stress and cognition," *Psychoneuroen-docrinology*, vol. 108, pp. 78–86, Oct. 2019.
- [51] H. A. Ingram, P. van Donkelaar, J. Cole, J.-L. Vercher, G. M. Gauthier, and R. C. Miall, "The role of proprioception and attention in a visuomotor adaptation task," *Exp. Brain Res.*, vol. 132, no. 1, pp. 114–126, Apr. 2000.
- [52] B. Hellwig, P. Mund, B. Schelter, B. Guschlbauer, J. Timmer, and C. H. Lücking, "A longitudinal study of tremor frequencies in Parkinson's disease and essential tremor," *Clin. Neurophysiol.*, vol. 120, no. 2, pp. 431–435, Feb. 2009.
- [53] C. Toth, M. Rajput, and A. H. Rajput, "Anomalies of asymmetry of clinical signs in parkinsonism," *Movement Disorders*, vol. 19, no. 2, pp. 151–157, Feb. 2004.
- [54] P. Mahlknecht, T. Foltynie, P. Limousin, and W. Poewe, "How does deep brain stimulation change the course of Parkinson's disease?" *Movement Disorders*, vol. 37, no. 8, pp. 1581–1592, Aug. 2022.
- [55] G. Ganga et al., "Longitudinal study of levodopa in Parkinson's disease: Effects of the advanced disease phase," *Movement Disorders*, vol. 28, no. 4, pp. 476–481, Apr. 2013.
- [56] J. Jankovic, "Parkinson's disease: Clinical features and diagnosis," J. Neurol. Neurosurg. Psychiatry, vol. 79, no. 4, pp. 368–376, 2008.
- [57] A. Winogrodzka et al., "Rigidity decreases resting tremor intensity in Parkinson's disease: A [123 I]β-CIT SPECT study in early, nonmedicated patients," *Movement Disorders*, vol. 16, no. 6, pp. 1033–1040, Nov. 2001.
- [58] R. C. Helmich, "The cerebral basis of parkinsonian tremor: A network perspective," *Movement Disorders*, vol. 33, no. 2, pp. 219–231, Feb. 2018.
- [59] T. E. Milner and C. Cloutier, "Damping of the wrist joint during voluntary movement," *Exp. Brain Res.*, vol. 122, no. 3, pp. 309–317, Sep. 1998.
- [60] D. Mitrovic, S. Klanke, R. Osu, M. Kawato, and S. Vijayakumar, "A computational model of limb impedance control based on principles of internal model uncertainty," *PLoS ONE*, vol. 5, no. 10, Oct. 2010, Art. no. e13601.
- [61] J. Ahn and N. Hogan, "Walking is not like reaching: Evidence from periodic mechanical perturbations," *PLoS ONE*, vol. 7, no. 3, Mar. 2012, Art. no. e31767.
- [62] P. Chen, R. Wang, D. Liou, and J. Shaw, "Gait disorders in Parkinson's disease: Assessment and management," *Int. J. Gerontol.*, vol. 7, no. 4, pp. 189–193, 2013.
- [63] R. L. Blakemore, M. R. MacAskill, D. J. Myall, and T. J. Anderson, "Volitional suppression of parkinsonian resting tremor," *Movement Disorders Clin. Pract.*, vol. 6, no. 6, pp. 470–478, Jul. 2019.
- [64] M. M. Carvalho et al., "Effect of levodopa on reward and impulsivity in a rat model of Parkinson's disease," *Frontiers Behav. Neurosci.*, vol. 11, p. 145, Aug. 2017.
- [65] Y. Worbe, G. Savulich, V. Voon, E. Fernandez-Egea, and T. W. Robbins, "Serotonin depletion induces 'waiting impulsivity' on the human four-choice serial reaction time task: Cross-species translational significance," *Neuropsychopharmacology*, vol. 39, no. 6, pp. 1519–1526, May 2014.
- [66] M. Politis and F. Niccolini, "Serotonin in Parkinson's disease," *Behav. Brain Res.*, vol. 277, pp. 136–145, Jan. 2015.